

# Melting Rate Analysis of the VP-GMAW Process

by

D.D. Harwig, J. Dierksheide, D. Yapp, and S. Blackman

## Abstract

The objective of this project was to determine the metal transfer behavior of the VP-GMAW process. Measurement techniques were developed to permit systematic study of the relationships between VP-GMAW waveform and metal transfer. A number of state-of-the-art VP-GMAW power supplies were evaluated on steel using mixed gas. A new melting rate measurement technique was developed using high-speed video and data acquisition. Here the droplet melting behavior was closely measured and related to the exact waveform parameter. These measurements accounted for the change in electrode extension during the droplet formation process, rather than assuming a constant electrode extension like the prior art. Measurements using this technique are believed to produce true material properties for the melting rate equation that was developed for VP-GMAW.

## Experimental Approach

The filler electrode was 1.2-mm (0.045-in.) diameter ER70S-6 uncoated steel wire used with 90%Ar-10%CO<sub>2</sub> shielding gas at 18.8 l/min. The majority of welding trials involved bead-on-plate and lap joint tests on sheet steel coupons. Moving table welding stations were fabricated to permit analysis of metal transfer using high-speed video that was synchronized with high-speed data acquisition (DAQ). A high-speed video (HSV) camera manufactured by Phantom was positioned to measure droplet transfer. The majority of tests performed in this investigation were performed using a frame speed of 3700 fps where the frame speed and shutter were adjusted to optimize the droplet image for different periods of the VP-GMAW waveform. This was required to accommodate the wide variation in light intensity from EP to EN current. The electrode extension neck position was closely measured and used in melting rate calculation with the wire feed speed.

## Droplet Burnoff Rate Measurement Technique

A droplet burnoff rate (DBR) measurement technique was developed that provided accurate melting rate measurements for advanced waveform processes, like VP-GMAW. This technique required detailed analysis of the electrical waveform and how it related to the droplet growth process for each period in the waveform. Drop volume melting rate ( $V_D$ ) during each period was determined empirically by high-speed image measurement using the following equation:

$$V_D = \left( \frac{\Delta x}{t_2 - t_1} + WFS_{DAQ} \right) \cdot A_w \quad (1)$$

Where  $\Delta x$  is the length of change in solid-liquid interface position from initial time ( $t_1$ ) to final time ( $t_2$ ) and WFS is wire feed speed. The change in interface position was measured by calibrating the high-speed video frames to the wire diameter (1.2-mm) and recording position at the initial and final times. The sign convention used for  $\Delta x$  required that positive interface growth be upward (toward the solid wire). Figure 1a shows the interface position at the beginning of the DCEN cycle. Figure 1b shows the interface position at the end of the DCEN cycle. In this case,

the time elapsed throughout the cycle is .01107 seconds and growth is in the positive direction ( $\Delta x > 0$ ).

The majority of melting rate measurements performed in this investigation were taken using the OTC AC/MIG 200 power supply. This VP-GMAW waveform (Figure 2) uses a trapezoidal EPP pulse with a small background (EPB) current after the ramp-down to permit drop transfer before switching to EN current. The melting rate equation for this power supply can be determined integrating the VP-GMAW waveform over time and assuming the ramp-up and ramp-down slew rates are equal. This was the case with the OTC AC/MIG 200 power supply. The resultant equation is the following:

$$MR_{vp} = \frac{\alpha_- |I_-| t_- + \alpha_+ \bar{I}_+ t_+}{t_- + t_+} + \beta \left\{ \frac{L_- I_-^2 t_-}{t} + L_+ \left[ \frac{\bar{I}_+^2 + \frac{(I_p - I_p)^2 t_p t_b}{(t_p + t_b)^2} - \frac{(I_p - I_b)^3}{3(t_p + t_b) dI/dt}}{t} \right] t_+ \right\} \quad (2)$$

For this project, the melting rate for each period of the waveform was empirically determined using the total WFS that were measured during droplet melting. The total WFS as a function of waveform period (EN, EPB, EPP) was determined based on dividing the  $V_D$  from Equation (1) by the area of the wire,  $A_w$ :

$$WFS_{T(EN, EPP, EPB)} = \frac{\Delta x}{t_2 - t_1} + WFS_{DAQ} \quad (3)$$

In order to empirically determine  $\alpha$  and  $\beta$  for different waveform periods, burn-off diagrams were plotted for each waveform period. The burn-off diagram plots burn-off rate ( $WFS_T/l$ ) versus the electrode extension times current ( $L \cdot I$ ), which is named the electrode extension heating factor ( $F_L$ ). Linear trend lines were fitted where the slope determines  $\beta$ , and the y-intercept determines  $\alpha$ . The coefficients measured for each waveform period were compared to prior art for EP heating, and used to establish the melting rate properties of EN heating.

The electrode extension-heating factor ( $F_L$ ) for each waveform period was determined as follows:

$$F_{L(EN, EPB, EPP)} = L \cdot I_{EN, EPB, EPP} \quad (4)$$

The electrode extension used in these calculations was the average based on the change in electrode extension length during the period of evaluation;

$$L_{EN, EPB, EPP} = L_0 \pm \frac{\Delta x}{2} \quad (5)$$

The average total wire feed speed for process stability can be determined by averaging the  $WFS_T$  for each period times the waveform frequency with the following equation:

$$WFS_{AVG} = \left( (WFS_{T(EN)} \cdot t_{EN}) + (WFS_{T(EPB)} \cdot t_{EPB}) + (WFS_{T(EPP)} \cdot t_{EPP}) \right) \cdot f \quad (6)$$

$WFS_{AVG}$  for each waveform should equal the true melting rate for that VP-GMAW waveform if the process is stable.

## Results and Discussion

Constant arc length and contact tip to work tests were used to study the effects of VP-GMAW waveform on melting rate. The power supply used in this investigation fixed the EP pulse period waveform, which was used to transfer globular droplets that were formed in the EN period. The EN current was proportional to the wire feed speed to maintain the melting rate. Setting the % EN on the pendant modified the waveform EN time and frequency. Pulse frequency was then trimmed, varying EP background time, to control arc length. The EN waveform can be used to reduce the heat input transferred to the work by over 25% compared to EP GMAW-P by increasing the EN current and time.

EN current and time were modified at several wire feed speeds to study EN waveform parameters. Five different wire feed speeds (42, 63, 84, 106, and 127 mm/sec) were characterized using the HSV technique at both low %EN (20-30%) and high %EN (65-75%). Drop volume melting rate was determined per equation (1) during the EN period. Graphs were plotted to evaluate how the EN drops grow over time, determine the magnitude of growth rate, and compare the effects of pulse parameters, Figure 3 and 4. These lines were made by measuring the detailed growth behavior of three drops and averaging the measurements.

Droplet growth in the EN period was linear for a given set of conditions. The slopes measured in these graphs had an average coefficient of multiple determination ( $R^2$ ) of 0.957, which indicated a good data fit. The effects of EN time at constant current can be made by comparing the droplet volume melting rate,  $V_D$  at constant current. The droplet growth was not linear with respect to EN time. At low EN time tests, Figure 3, the droplet volume melting rates were higher compared high EN time tests performed at the same current.

Melting rate measurements were made by plotting the burnoff diagram using DBR technique described above. Here, the  $WFS_T$  was determined for five different wire feed speeds (42, 63, 84, 106, and 127 mm/sec) using six different %EN levels that varied from 0 to 75%. Approximately, twenty drops were measured to determine an average  $WFS_T$ ,  $L_F$ , and EN current and time at each condition. These results were plotted to construct the burnoff diagram (Figure 5), which was used to solve for the melting rate coefficients. Burnoff diagrams for a given electrode type and diameter are usually linear for EP regardless of pulse waveform. In these results, the EN waveform was found to produce higher slopes with shorter EN periods at constant current. Comparing the equations that were solved for each line shows that the slope ( $\beta$ ) varies from  $2.9$  to  $6.0 \times 10^{-4} \text{ amps}^{-2}\text{sec}^{-1}$ . For EP GMAW-P, the resistive heating coefficient has been found to equal between  $3.5$  to  $3.74 \times 10^{-4} \text{ amps}^{-2}\text{sec}^{-1}$  (Ref. 1). The EN  $\beta$  values were equivalent to GMAW-P  $\beta$  values with the higher EN time tests.

The arc heating coefficients (intercepts in Figure 5) were significant. Average  $\alpha$  was approximately  $0.8 \text{ amps}^{-1}\text{sec}^{-1}$  versus  $0.55 \text{ amps}^{-1}\text{sec}^{-1}$  that has been measured for steel using GMAW-P (Ref. 1). The slope of the lines for EN burnoff diagram varied little. The small variation was attributed to the grouping of EN time in 3 msec groups, which was the range for each EN current for each WFS and %EN combination. This was due to frequency trim

adjustments to acquire the test arc length. Overall, the EN polarity was found to provide 45% more arc heating than EP polarity.

A theory was developed to explain why  $\beta$  was greater for short EN time compared to EP. The increase in melting rate at short EN times was believed to be due to a burst heating effect. Careful observation of the HSV data showed that drops form by melting the electrode tip, which consumes the electrode extension rapidly once in the EN period. The electrode extension burnoff was seen to saturate as the EN time increased at constant current and wire feed speed. The large drop that was formed decreased the effect of cathode heating since the arc rooted on it, probably superheating the drop. This effect increased the resistance heating coefficient (slope) since the electrode extension burnback was substantial at short EN times relative to longer EN times.

### **Conclusions**

1. The DBR method for measuring melting rate properties was found to give accurate measurements of advanced waveform processes, like VP-GMAW.
2. The arc heating coefficient,  $\alpha$  for EN was 45% greater than EP polarity in the VP-GMA welding of steel.

### **References**

1. Richardson, et al. "The Influence of Power Supply Dynamics on Wire Melting Rate in Pulsed GMA Welding" *Welding Journal*, Feb 1994.

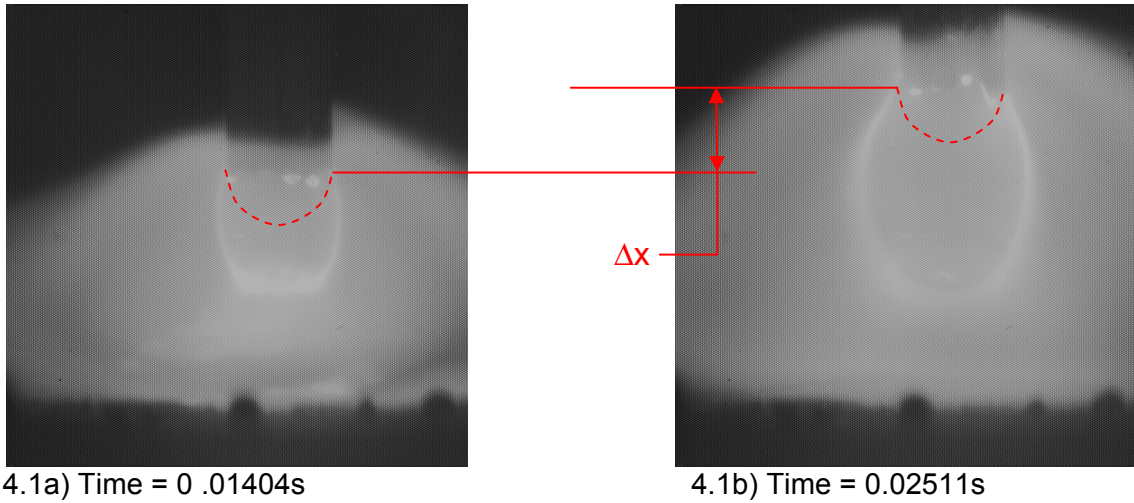


**Figure 1. Electrode Extension Burnoff During Droplet Growth with EN Current Waveform Period**

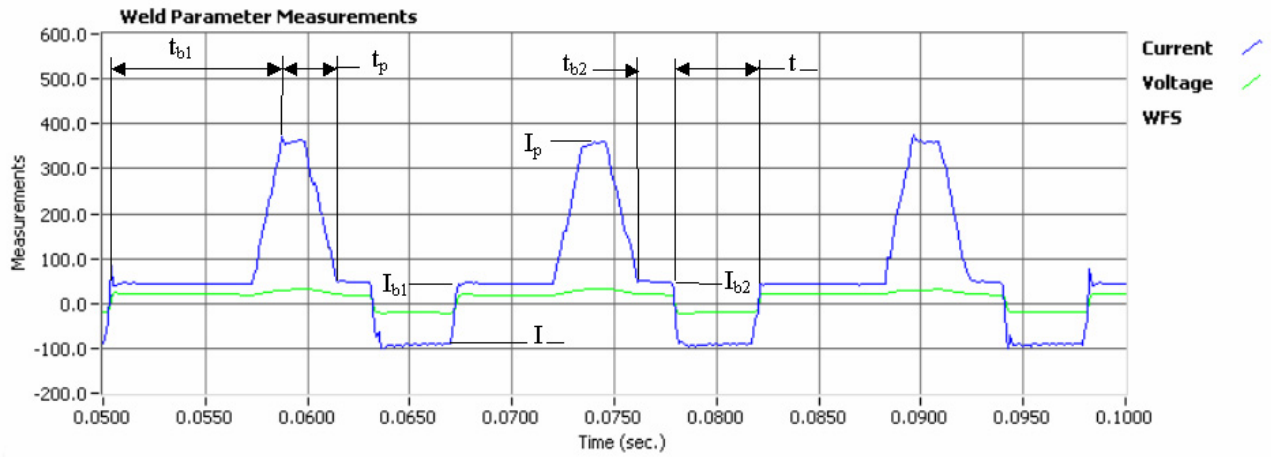


**Figure 2. Typical Waveforms for AC/MIG 200 Power Supply**

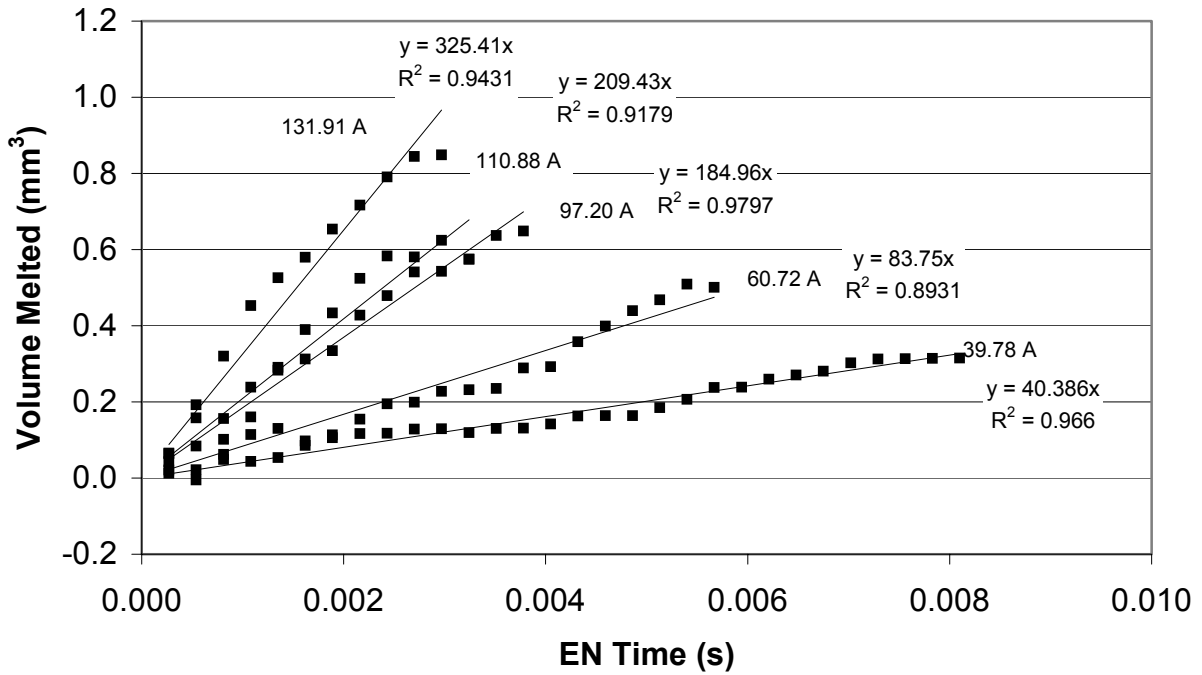


Figure 3. Drop Volume vs. Low EN Time at Different WFS's and EN Currents

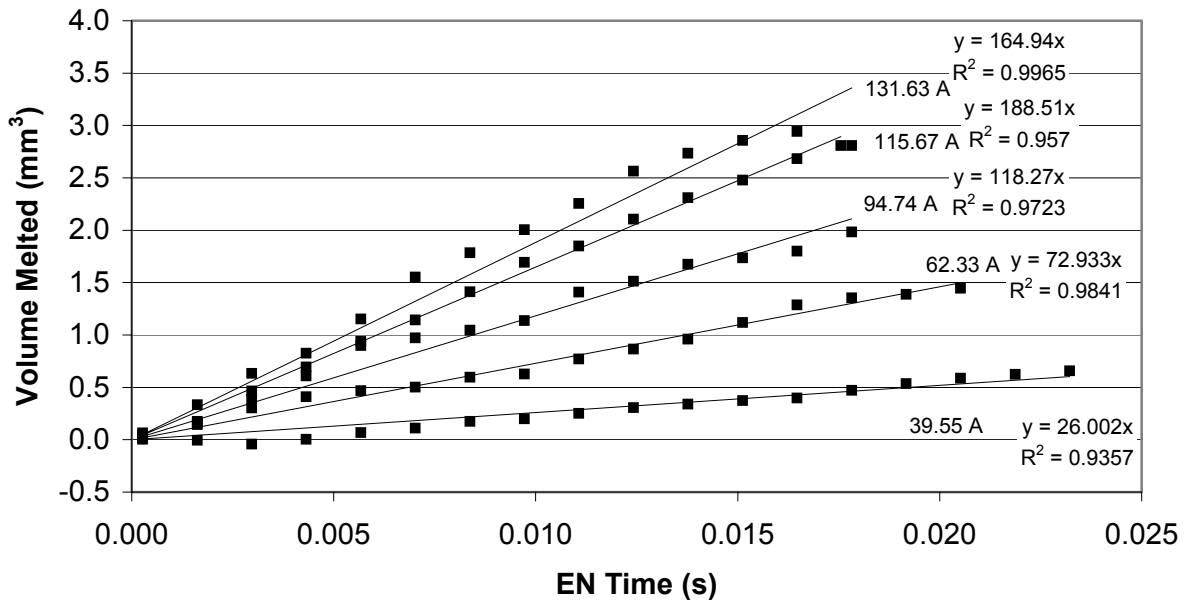
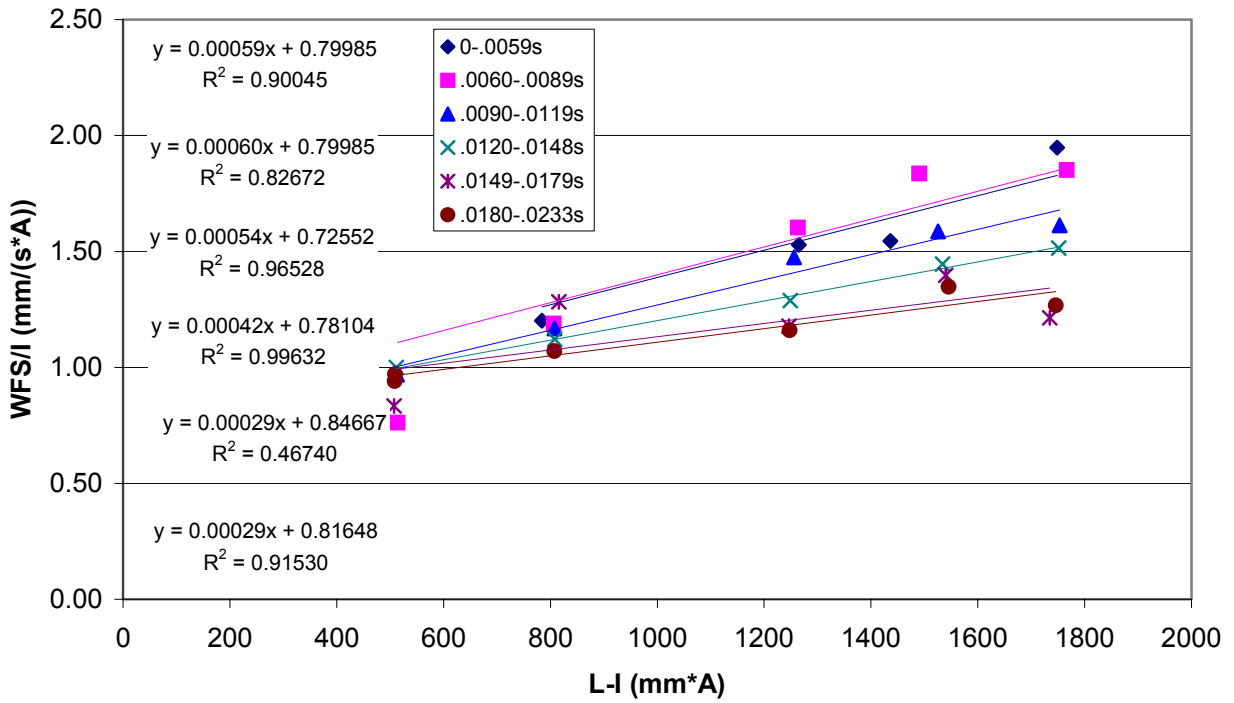


Figure 4. Drop Volume vs. High EN Time at Different WFS's and EN Currents



**Figure 5. Burnoff Rate vs. Electrode Extension Heating Factor** (line slope equals  $\beta$  and the intercept equals  $\alpha$  )